*Safety, Reliability, Risk and Life-Cycle Performance of Structures & Infrastructures – Deodatis, Ellingwood & Frangopol (Eds)*
*© 2013 Taylor & Francis Group, London, ISBN 978-1-138-00086-5*

# Resilience of concrete frame structures under corrosion

A. Titi & F. Biondini
*Department of Civil and Environmental Engineering, Politecnico di Milano, Milan, Italy*

ABSTRACT: This paper presents a probabilistic approach to lifetime assessment of seismic resilience of deteriorating concrete structures. The effects of environmental damage on the seismic performance are evaluated by means of a methodology for lifetime assessment of concrete structures exposed to aggressive environments. The time-variant seismic capacity associated to different limit states, from damage limitation up to collapse, is assumed as functionality indicator and seismic resilience is evaluated with respect to this indicator over the structural lifetime. The effectiveness of the proposed approach is shown through the application to a precast concrete frame under corrosion. The results show that structures designed for the same functionality target could exhibit over time different seismic resilience depending on the environmental exposure.

## 1 INTRODUCTION

The concept of resilience is becoming increasingly important in design, assessment, maintenance and rehabilitation of structure and infrastructure systems. In general, resilience can be related to the capability of a system, a community or a society, to withstand the effects of extreme events and to recover efficiently the original performance and functionality (Bruneau *et al.* 2003). Resilience of critical facilities, such as hospitals and infrastructure networks, is often investigated with reference to damage and disruption caused by seismic events (Bruneau *et al.* 2003, Chang & Shinozuka 2004, Bruneau & Reinhorn 2007, Cimellaro *et al.* 2010a, 2010b, Bocchini & Frangopol 2012, Bocchini *et al.* 2012, Decò *et al.* 2013). However, for structural systems damage could also arise progressively in time due to aging and environmental aggressiveness, which can modify over time the structural performance and functionality and, consequently, the system resilience. In particular, for concrete structures the exposure to aggressive agents, such as chlorides, may involve corrosion of reinforcement and affect over time the structural resilience. This is important also for precast systems, for which most of the structural members are often directly exposed to the atmosphere and environmental aggressiveness (Biondini *et al.* 2011).

This paper presents a probabilistic approach to lifetime assessment of seismic resilience of concrete structures considering the interaction of seismic and environmental hazards. The proposed approach is based on a general methodology for lifetime assessment of concrete structures exposed to aggressive environments (Biondini *et al.* 2004, 2006, 2013, Biondini & Frangopol 2009). The role of the environmental damage on seismic resilience is investigated by comparing the system functionality in the original state, in which the structure is fully intact, and in a perturbed state, in which a damage scenario is applied (Frangopol & Curley 1987, Biondini 2009). The time-variant seismic capacity associated to different limit states, from damage limitation up to collapse, is assumed as functionality indicator and seismic resilience is evaluated with respect to this indicator over the structural lifetime.

The effectiveness of the proposed approach is shown through the application to probabilistic assessment of seismic resilience of a precast concrete frame under corrosion. The results show that structures designed for the same functionality target could exhibit over time different seismic resilience depending on the environmental exposure. This emphasizes the importance of a life-cycle approach to the assessment of seismic resilience of deteriorating structures.

## 2 LIFETIME SEISMIC RESILIENCE

### 2.1 *Time-variant resilience*

Let $Q = Q(t)$ be a time-variant functionality indicator in the range [0,1], with $Q = 1$ for undamaged systems and $Q = 0$ for fully damaged systems. The occurrence of an extreme event at time $t_0$ may cause a sudden loss $\Delta Q$ of system functionality. The loss $\Delta Q$ can be totally or partially recovered by post-event restoration activities over a recovery time interval $\Delta t = t_f - t_i$, where $t_i \geq t_0$ and $t_f$ are the initial and final time of the restoration process, respectively. Resilience can be defined as the capability of the system to sustain the effects $\Delta Q$ of the extreme event and to recover efficiently a target level of functionality. Based on this definition, an effective dimensionless measure of resilience is given

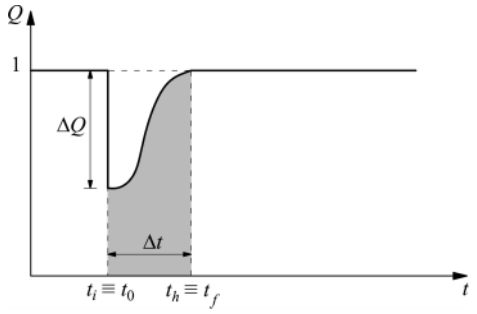


Figure 1. Functionality $Q$ of non deteriorating systems: functionality loss $\Delta Q$ due to the occurrence of an extreme event at time $t_0$ and recovery over the time interval $\Delta t = t_f - t_i$ ($t_i = t_0$, $t_h = t_f$).

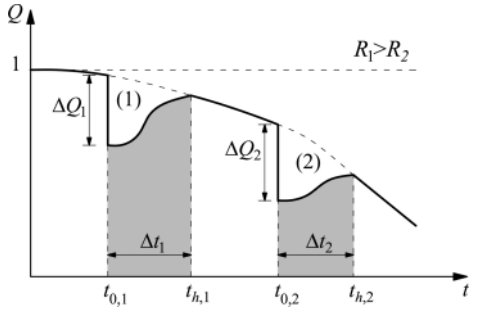


Figure 2. Functionality $Q$ of deteriorating systems: functionality losses $\Delta Q_k$ due to the occurrence of extreme events $k = 1,2,\ldots$, at different times $t_{0,k}$ and recovery over the time intervals $\Delta t_k$.

by an average value of the post-event functionality over a time horizon $t_h \geq t_f$ (Bocchini *et al.* 2012):

$$R = \frac{1}{t_h - t_0} \int_{t_0}^{t_h} Q(t)dt \tag{1}$$

This concept is shown in Figure 1 for $t_i = t_0$ and $t_h = t_f$.

Resilience is generally investigated by assuming a time-invariant functionality before the occurrence of an extreme event, and after the completion of the restoration process, as shown in Figure 1. According to this assumption, resilience depends only on the recovery profile $Q = Q(t)$ over the time interval $[t_0, t_h]$ and it is independent of the time $t_0$ of occurrence of the extreme event. However, the effects of damage due to aging and environmental aggressiveness could reduce over time the system functionality. Consequently, for deteriorating structural systems the resilience depends also on the time $t_0$ when the extreme event occurs, as shown in Figure 2. A lifetime assessment of resilience is therefore necessary for structural systems exposed to damage.

It is worth noting that the lifetime structural resilience $R = R(t_0)$ may depend on several factors related to the deterioration process, including the level of exposure to environmental aggressiveness (Figure 3.a), the effectiveness of post-event recovery actions, which may involve a total or partial restoring of the initial functionality of the undamaged system (Figure 3.b), and the effects of maintenance interventions (Figure 3.c).

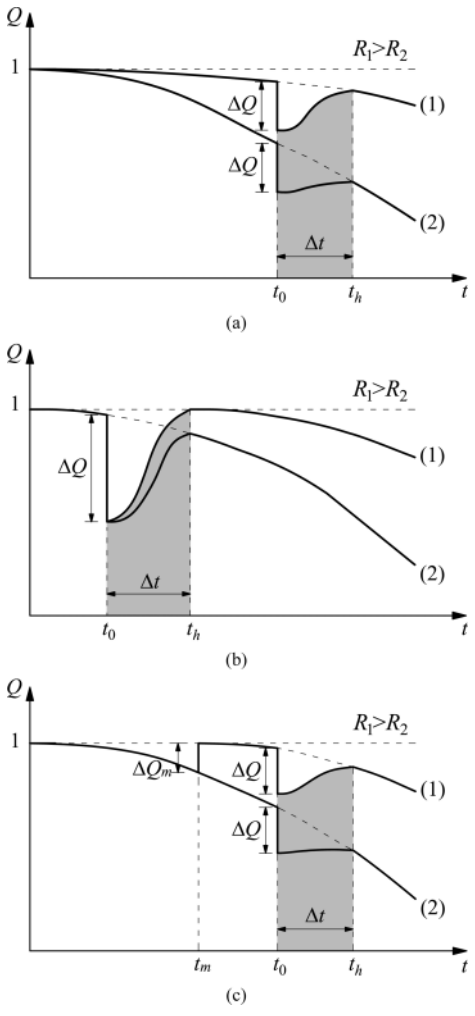


Figure 3. Effects of the deterioration process and related factors on system functionality $Q = Q(t)$ and lifetime resilience $R = R(t_0)$. (a) Environmental aggressiveness with (1) slight/ moderate exposure or (2) severe exposure. (b) Post-event recovery actions with (1) total restoring of the initial functionality or (2) partial restoring of the pre-event functionality. (c) Maintenance programs (1) with and (2) without maintenance interventions.

## 2.2 *Functionality indicator*

Several indicators can be chosen to effectively represent the system functionality. In this paper, the lifetime resilience of concrete frame buildings under corrosion is investigated with reference to the possible occurrence of seismic events. In this context, the functionality is affected by both corrosion deterioration and seismic damage and should be related to the

residual seismic capacity of the structure. Depending on the type of building, this relationship may be non-linear and involve the definition of seismic capacity thresholds and discrete functionality states. These are important issues that should be addressed by future research. For the purpose of the present study, the residual seismic capacity in terms of peak ground acceleration $a_g$ associated to the reaching of prescribed limit states, from damage limitation up to collapse, is assumed as time-variant functionality indicator:

$$Q(t) = \frac{a_g(t)}{a_{g0}} \tag{2}$$

where the seismic capacity $a_g = a_g(t)$ of the deteriorated system at time $t$ is normalized to the seismic capacity $a_{g0} = a_g(0)$ of the undamaged system at time $t = 0$.

### 2.3 *Recovery profiles*

A functionality recovery model can be effectively represented as follows:

$$Q(\tau) = Q_r + H(\tau) r(\tau) (Q_t - Q_r) \tag{3}$$

where $Q_r$ is the residual functionality at the initial time $t = t_i$ of the recovery process, $Q_t$ is the target functionality at the end of the recovery time interval $\Delta t = t_f - t_i$, $\tau = (t - t_i)/\Delta t \in [0,1]$ is a normalized time variable, $H = H(\tau)$ is the Heaviside unit step function, and $r = r(\tau) \in [0,1]$ is a recovery function.

The functionality recovery profile depends on many factors, including type of system and components, type, magnitude and location of damage, and restoring techniques (Bocchini *et al.* 2012, Decò *et al.* 2013). Effective functionality recovery models have been proposed by Kafali & Grigoriu (2005), Cimellaro *et al.* (2010b), Bocchini *et al.* (2012). In this paper, the role of the recovery process on the lifetime seismic resilience is investigated by considering the following three recovery functions:

$$r(\tau) = e^{-k(1-\tau)} \qquad \text{negative-exponential} \tag{4}$$

$$r(\tau) = \frac{1 - \cos(\pi\tau)}{2} \qquad \text{sinusoidal} \tag{5}$$

$$r(\tau) = 1 - e^{-k\tau} \qquad \text{positive-exponential} \tag{6}$$

where $k$ is a shape parameter. Figure 4 shows the three recovery models for $k = 10$. A negative-exponential-type function can reproduce recovery processes where most of functionality is restored quickly after the seismic event. A sinusoidal-type function describes a recovery process where functionality is restored gradually in time. Finally, a positive-exponential-type function can represent recovery processes where functionality is restored mainly at the end of the recovery time interval.

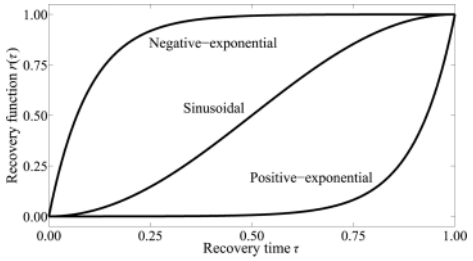


Figure 4. Recovery functions ($k = 10$).

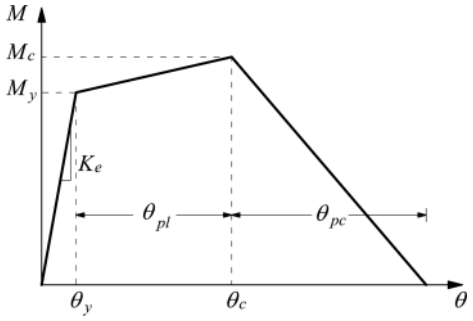


Figure 5. Bending moment $M$ vs rotation $\theta$ envelope curve.

## 3 SEISMIC ASSESSMENT

### 3.1 *Structural modelling*

The structural modelling for the assessment of seismic performance is based on beam finite elements with material non-linearity lumped at the beam ends, where plastic hinges are expected to occur. The non-linear behaviour of the plastic hinges is defined in terms of bending moment $M$ vs rotation $\theta$ relationships. The cyclic model proposed by Ibarra *et al.* (2005) is adopted, with the tri-linear envelope curve shown in Figure 5. The parameters of the limit points of the envelope curve are evaluated by using the calibration equations proposed by Haselton (2006). Further details can be found in Titi (2012).

### 3.2 *Limit states*

The seismic capacity is evaluated with reference to different limit states. At the element level (Figure 5) the following limit states are defined (Dolšek 2011):

- Damage Limitation (DL): limit state associated to the yielding point, with rotation $\theta = \theta_y = M_y/K_e$;
- Significant Damage (SD): limit state associated to the capping point, with rotation $\theta = \theta_c$;
- Near Collapse (NC): limit state associated to the ultimate point corresponding to a bending moment $M_u = 0.8M_c$ with rotation $\theta = \theta_u > \theta_c$.

At the structural level, the DL limit state is attained when all columns at any storey of the concrete frame

reach the DL limit state. The SD and NC limit states are instead attained when one of the columns reaches the corresponding limit state. However, if the NC base shear is lower than 80% of the maximum base shear capacity, such limits are relaxed. In this case the NC limit state is related to a post-peak drop of 20% of the base shear with respect to the maximum base shear capacity, and the SD limit state is defined at the 75% of the NC top displacement (Dolšek 2011).

### 3.3 *Seismic capacity*

The seismic capacity of concrete frames with respect to the DL, SD, and NC limit states is evaluated by means of non-linear static analysis based on the N2 method (Fajfar 1999). The effects of seismic damage are instead reproduced by non-linear dynamic time-history analysis under prescribed ground motion. In this way, the residual seismic capacity $a_g = a_g(t)$ after occurrence of a seismic event can be evaluated by performing a non-linear static analysis in sequence to a non-linear dynamic time-history analysis.

## 4 STRUCTURAL DETERIORATION

A lifetime performance analysis of concrete structures in aggressive environments should account for both the diffusion process of the aggressive agents, such as chlorides, and the mechanical damage induced by diffusion, which usually involves corrosion of reinforcement (Bertolini *et al.* 2004).

### 4.1 *Diffusion process*

The diffusion process is described by the Fick's laws which, for single component diffusion in isotropic, homogeneous and time-invariant media, can be reduced to the following second order partial differential linear equation (Glicksman 2000):

$$D\nabla^2 C = \frac{\partial C}{\partial t} \tag{7}$$

where $D$ is the diffusivity coefficient of the medium, $C = C(\mathbf{x}, t)$ is the concentration of the chemical component at point $\mathbf{x}$ and time $t$, $\nabla C = \mathbf{grad}\ C(\mathbf{x}, t)$ and $\nabla^2 = \nabla \cdot \nabla$. The numerical solution of the Fick's differential equations is achieved by means of cellular automata (Biondini *et al.* 2004, 2006).

### 4.2 *Damage index*

Damage induced by diffusion is studied by considering the effects of uniform corrosion in terms of mass loss of the reinforcing steel bars. The percentage loss of steel resistant area for a corroded steel bar is described by means of a dimensionless damage index $\delta_s = \delta_s(t)$ which provides a direct measure of damage within the range [0,1]. The corrosion rate depends on the concentration $C = C(\mathbf{x}, t)$ of the chemical substance. Despite the complexity of the problem, available data for sulphate and chloride attacks (Pastore & Pedeferri 1994) indicates that a linear dependency can be reasonably assumed (Biondini *et al.* 2004):

$$\frac{\partial \delta_s(t)}{\partial t} = \rho\, C(\mathbf{x}, t) \tag{8}$$

where $\rho$ is a steel damage rate coefficient.

Table 1. Probability distributions and coefficients of variation.

| Random Variable ($t = 0$) | Distribution | C.o.V. |
|---|---|---|
| Mass, $m$ | Normal (*) | 0.10 |
| Concrete strength, $f_c$ | Lognormal | 5 MPa/$f_{c,m}$ |
| Steel strength, $f_{sy}$ | Lognormal | 30 MPa/$f_{sy,m}$ |
| Initial stiffness, $K_e$ | Lognormal | 0.28 |
| Capping to yielding bending moment ratio, $M_c/M_y$ | Lognormal | 0.10 |
| Capping rotation, $\theta_c$ | Lognormal | 0.45 |
| Post-capping rotation, $\theta_{pc}$ | Lognormal | 0.72 |
| Energy dissipation capacity, $\lambda$ | Lognormal | 0.49 |
| Diffusivity, $D$ | Normal (*) | 0.10 |
| Steel damage rate, $\rho$ | Normal (*) | 0.30 |

(*)Truncated distributions with non negative outcomes.

## 5 PROBABILISTIC MODELING

The time-variant system functionality $Q = Q(t)$ and lifetime seismic resilience $R = R(t_0)$ are affected by uncertainty and have to be investigated in probabilistic terms. To this aim, a lifetime probabilistic analysis is carried out by Monte Carlo simulation based on a probabilistic modelling of the diffusion process and damage propagation of concrete members exposed to corrosion (Biondini *et al.* 2006).

The probabilistic model assumes the following quantities as random variables: mass $m$ at each storey; concrete compression strength $f_c$; steel yielding strength $f_{sy}$; initial stiffness $K_e$; ratio of capping moment to yielding moment $M_c/M_y$; rotation at capping point $\theta_c$; rotation of the post-capping branch $\theta_{pc}$; energy dissipation capacity $\lambda$; diffusivity coefficient $D$; steel damage rate $\rho$. These variables are assumed uncorrelated with the probabilistic distribution and coefficients of variation listed in Table 1 (Biondini *et al.* 2006, Haselton 2006, Dolšek 2009).

The Monte Carlo simulation is performed by Latin Hypercube Sampling (Iman & Conover 1982) with correlation control based on a Simulated Annealing method (Vořechovský & Novák 2009).

## 6 APPLICATION

### 6.1 *Two-storey precast concrete frame*

The two-storey precast concrete frame with pinned beam-to-column joints shown in Figure 6 is considered. The nominal effective weight at each storey is $w = mg = 1200$ kN. The nominal material strengths are $f_c = 48$ MPa and $f_{sy} = 450$ MPa. The parameters of

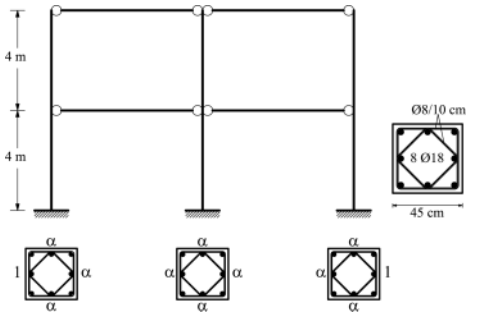


Figure 6. Two-storey precast concrete frame with pinned joints. Structural geometry, columns cross-section, and damage scenario with exposure levels ($0 \le \alpha \le 1$).

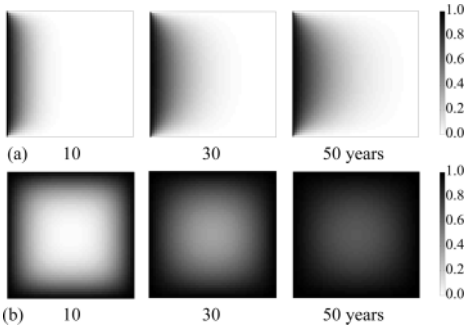


Figure 7. Maps of the concentration $C(\mathbf{x},t)/C_0$ of the aggressive agent for a lateral column after 10, 30, and 50 years from the initial time of diffusion penetration: (a) $\alpha = 0$; (b) $\alpha = 1$ (Figure 6).

the cyclic model (Figure 5) are computed by using the calibration equations proposed by Haselton (2006).

### 6.2 *Time-variant seismic capacity*

The concrete frame is subjected to a diffusive attack from chlorides located on the external surfaces of the columns. The exposure scenario shown in Figure 6 is considered, with concentration $C_0 = 3\%$ [wt.%/c] on the outermost side of the two lateral columns and $\alpha C_0$ on all other column sides. A nominal diffusivity coefficient $D = 10^{-11}$ m$^2$/sec is assumed. Figure 7 shows the maps of concentration $C(\mathbf{x},t)/C_0$ of a lateral column for two exposure levels, with $\alpha = 0$ and $\alpha = 1$, after 10, 30, and 50 years from the initial time of diffusion penetration.

The corrosion damage induced by diffusion is evaluated by assuming a nominal damage rate coefficient $\rho C_0 = 0.02$ sec$^{-1}$, with corrosion initiation associated to a critical threshold of concentration $C_{cr} = 0.6\%$ [wt.%/c]. The values of seismic capacity $a_g = a_g(t)$ at DL, SD, and NC limit states for the two exposure scenarios shown in Figure 7, with $\alpha = 0$ and $\alpha = 1$, are listed in Table 2. It can be noted that the deterioration process leads to a remarkable reduction of seismic capacity over time, with drops up to 18% for $\alpha = 0$ and 61% for $\alpha = 1$ after 50 years of lifetime.

Table 2. Seismic capacity $a_g$ [g] at DL, SD, and NC limit states for the two exposure scenarios with $\alpha = 0$ and $\alpha = 1$ (Figure 7).

| $t$ | $\alpha = 0$ | | | $\alpha = 1$ | | |
|---|---|---|---|---|---|---|
| [years] | DL | SD | NC | DL | SD | NC |
| 0 | 0.109 | 0.155 | 0.205 | 0.109 | 0.155 | 0.205 |
| 10 | 0.105 | 0.151 | 0.201 | 0.101 | 0.147 | 0.197 |
| 30 | 0.100 | 0.142 | 0.189 | 0.084 | 0.122 | 0.165 |
| 50 | 0.095 | 0.127 | 0.169 | 0.043 | 0.081 | 0.111 |

### 6.3 *Probabilistic lifetime seismic resilience*

A probabilistic analysis is performed based on the probabilistic parameters given in Table 1 and by assuming the three sets of random variables associated to each column as fully correlated. The results of the simulation process are firstly discussed for the NC limit state and exposure scenario with $\alpha = 1$. Figure 8 shows the evolution during the simulation process of the probabilistic parameters of the seismic capacity $a_g = a_g(t)$ at the initial time $t = 0$ and after 50 years of lifetime for a sample of 1000 realizations. Figure 9 shows the corresponding probability mass functions (PMFs) based on a sample of 3000 realizations.

The time evolution of the probabilistic parameters of the system functionality $Q = Q(t)$ associated to the residual seismic capacity $a_g = a_g(t)$ is shown in Figure 10. These results indicate that, over time, the mean value of functionality decreases and the effects of uncertainty increase due to the deterioration process. Therefore, the probability distribution of seismic resilience $R = R(t_0)$ depends on the time $t_0$ of occurrence of the seismic event, as shown in Figure 11 for $t_i = t_0$, $t_h = t_f$, functionality loss $\Delta Q(t_0) = 0.5Q(t_0)$, and recovery process with sinusoidal profile and partial restoring aimed to recover the pre-event functionality (see Figure 3.b). It is worth noting that, under the assumptions of negligible idle time between the occurrence of the seismic event and the beginning of the recovery process ($t_i = t_0$) and time horizon limited to the final recovery time ($t_h = t_f$), the lifetime seismic resilience does not depend significantly on the recovery time interval $\Delta t = t_f - t_i$. As an example, for the case studied, the variation of the mean value of seismic resilience does not exceed 1% for recovery time intervals up to $\Delta t = 60$ months at $t = 0$, and $\Delta t = 12$ months at $t = 50$ years. However, the influence of the recovery time becomes important when the idle time and wider time horizons are considered.

### 6.4 *Influence of main factors on lifetime resilience*

The role of the main factors affecting the lifetime seismic resilience, including the level of exposure $\alpha$, the loss of functionality $\Delta Q$, the functionality target $Q_t$, the recovery profile $r = r(\tau)$, and the limit states DL, SD, NC, is investigated. The results are shown in Figures 12 to 15. It is noted that the level of exposure to environmental aggressiveness (Figure 12) and the

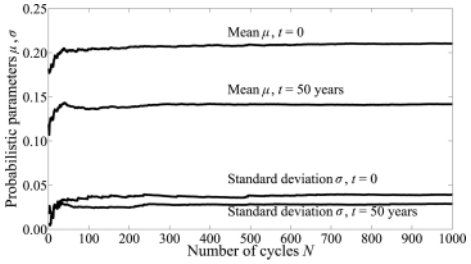


Figure 8. Evolution during the simulation process of the mean value $\mu$ and standard deviation value $\sigma$ of the seismic capacity $a_g$ [g] at NC limit state for the exposure scenario with $\alpha = 1$ at the initial time $t = 0$ and after 50 years of lifetime.

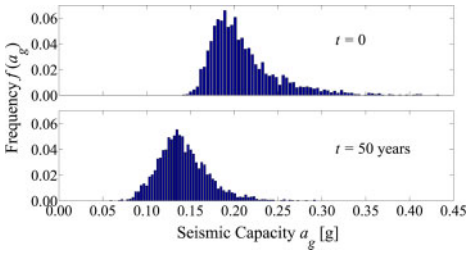


Figure 9. PMFs of the seismic capacity $a_g = a_g(t)$ at the NC limit state for the exposure scenario with $\alpha = 1$ at the initial time $t = 0$ and after 50 years of lifetime (3000 realizations).

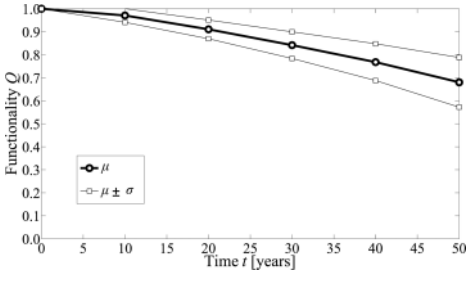


Figure 10. Time evolution of the probabilistic parameters of the system functionality $Q = Q(t)$ at NC limit state for $\alpha = 1$.

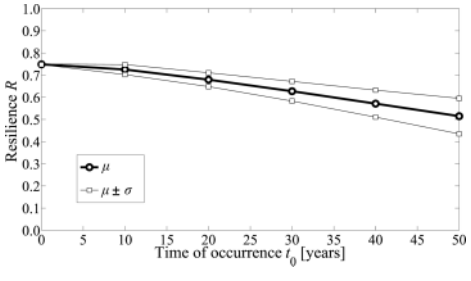


Figure 11. Time evolution of the probabilistic parameters of the seismic resilience $R = R(t_0)$: NC limit state, $\alpha = 1$, $\Delta Q(t_0) = 0.5Q(t_0)$, partial restoring, sinusoidal recovery profile.

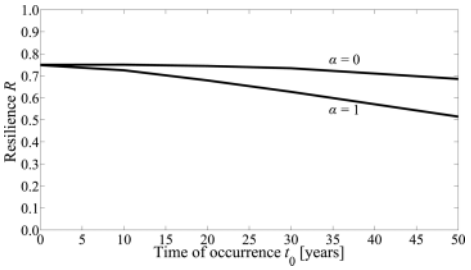


Figure 12. Mean value of seismic resilience $R = R(t_0)$ for the two exposure levels $\alpha = 0$ and $\alpha = 1$: NC limit state, $\Delta Q(t_0) = 0.5Q(t_0)$, partial restoring, sinusoidal recovery profile.

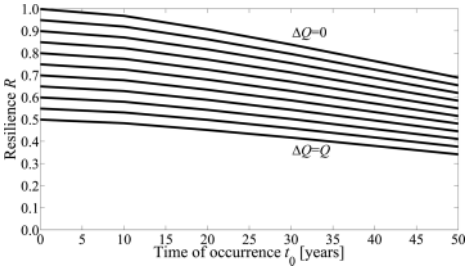


Figure 13. Mean value of seismic resilience $R = R(t_0)$ for different levels of functionality loss, from $\Delta Q(t_0) = 0$ to $\Delta Q(t_0) = Q(t_0)$ with steps $0.1Q(t_0)$: NC limit state, $\alpha = 1$, partial restoring, sinusoidal recovery profile.

expected loss of functionality due to seismic events (Figure 13) may significantly affect the lifetime seismic resilience. This highlights the crucial importance of a proper modelling of both the lifetime deterioration process and the damage effects due to seismic events. The functionality target of the recovery process is also an important factor to improve the lifetime seismic resilience and to reduce the time effects of both deterioration and seismic damage (Figure 14). The type of recovery profile is one the most important factor to ensure suitable levels of lifetime seismic resilience (Figure 15). However, the role of deterioration on lifetime resilience is not modified by the type of recovery process, since the ratio $R(t_0)/R(0)$ is almost independent of the recovery profile. Finally, similar values of lifetime resilience are obtained for the three limit states DL, SD, and NC (see Figure 11).

### 6.5 *Time-variant effects of seismic damage*

The loss of functionality $\Delta Q = \Delta Q(t_0)$ is due to the effects of seismic damage and may vary over time due to the deterioration process. The combined effects of seismic damage and deterioration are investigated with reference to the NC limit state with exposure $\alpha = 1$ and by assuming a recovery process with partial restoring and sinusoidal recovery profile. Seismic damage is reproduced by non-linear dynamic time-history analyses under artificial accelerograms generated to be compatible with the elastic response

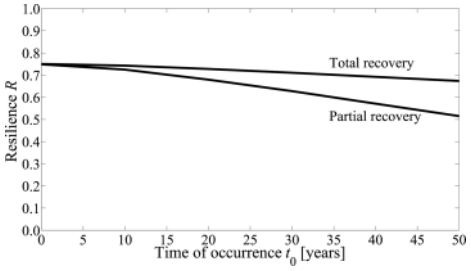


Figure 14. Mean value of seismic resilience $R = R(t_0)$ for total restoring of the initial functionality, and partial restoring of the pre-event functionality (see Figure 3.b): NC limit state, $\alpha = 1$, $\Delta Q(t_0) = 0.5Q(t_0)$, sinusoidal recovery profile.

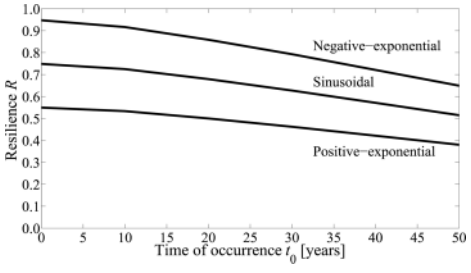


Figure 15. Mean value of seismic resilience $R = R(t_0)$ for negative-exponential, sinusoidal, and positive-exponential recovery profiles: NC limit state, $\alpha = 1$, $\Delta Q(t_0) = 0.5Q(t_0)$, partial restoring.

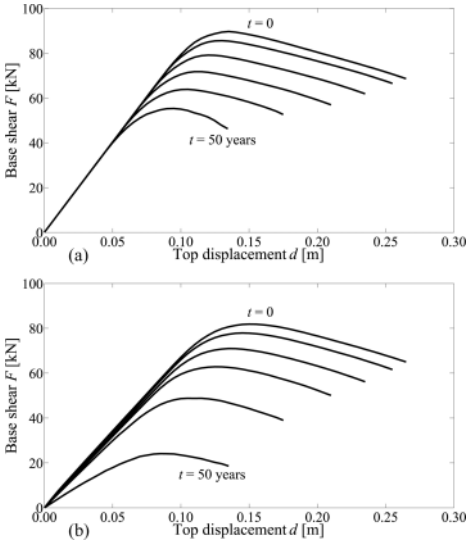


Figure 16. Time evolution of the mean base shear vs top displacement capacity curves for $\alpha = 1$ over 50 years of lifetime, with steps of 10 years. (a) Effects of corrosion. (b) Combined effects of corrosion and seismic damage.

spectrum of Eurocode 8 for soil type B (CEN-EN 1998-1 2004) with $a_{g,max} = 0.15$ g. Figure 16 shows the time evolution of the mean base shear vs top displacement capacity curves over 50 years of lifetime

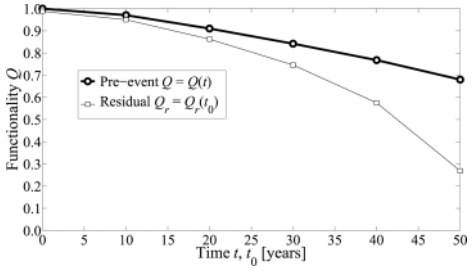


Figure 17. Time evolution of the mean values of functionality $Q = Q(t)$ of the corroded structure and residual functionality $Q_r = Q_r(t_0)$ associated to the combined effects of corrosion and seismic damage, evaluated at NC limit state for $\alpha = 1$.

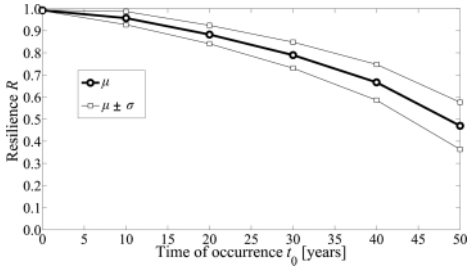


Figure 18. Time evolution of the probabilistic parameters of the seismic resilience $R = R(t_0)$ for a functionality loss $\Delta Q = \Delta Q(t_0)$ associated to time-variant seismic damage: NC limit state, $\alpha = 1$, partial restoring, sinusoidal recovery profile.

by considering only the effects of corrosion (Figure 16.a), as well as the combined effects of corrosion and seismic damage (Figure 16.b). These diagrams clearly highlight the influence of deterioration on the effects of seismic damage. The remarkable increase over time of such effects is also shown in Figure 17, where the mean values of functionality $Q = Q(t)$ of the corroded structure and residual functionality $Q_r = Q_r(t_0)$ after seismic damage, are compared. The time evolution of the probabilistic parameters of seismic resilience is finally shown in Figure 18. The comparison with the results shown in Figure 11 demonstrates the importance of a proper evaluation of the combined effects of seismic damage and deterioration process.

## 7 CONCLUSIONS

A probabilistic methodology for lifetime assessment of seismic resilience of concrete structures has been presented. Based on the proposed approach, it has been shown that the effects of corrosion damage due to aggressive agents, such as chlorides, may reduce over time the system functionality and, consequently, make the seismic resilience depending on the time of occurrence of the seismic event. The main factors affecting the time evolution of seismic resilience are the deterioration process and the combined effects of

deterioration and seismic damage. In fact, the results of the presented application demonstrated that the same structure may exhibit over time different seismic resilience depending on the environmental exposure, and that the loss of functionality due to seismic damage may change over time due to the deterioration process. These results highlight the need of a proper evaluation of the combined effects of seismic damage and deterioration process and emphasize the importance of a life-cycle approach to the assessment of seismic resilience of deteriorating structures.

There are relevant issues that should be addressed by future research, such as the formulation of non-linear functionality indicators based on seismic capacity thresholds and/or discrete functionality states, and the implementation of recovery functions with time-variant parameters related to type, magnitude, and location of damage. Moreover, the role of several factors and of the related uncertainty should be further investigated, including idle time, recovery time, target functionality, and time horizon. The effects of maintenance and repair interventions also need to be incorporated in the proposed probabilistic framework for the lifetime assessment of seismic resilience.

## REFERENCES


Bertolini, L., Elsener, B., Pedeferri, P. & Polder, R. 2004. *Corrosion of Steel in Concrete*. Wiley-VCH, Weinheim, Germany.

Biondini, F., Bontempi, F., Frangopol, D.M. & Malerba, P.G. 2004. Cellular Automata Approach to Durability Analysis of Concrete Structures in Aggressive Environments, *Journal of Structural Engineering*, ASCE, 130(11), 1724–1737.

Biondini, F., Bontempi, F., Frangopol, D.M. & Malerba, P.G. 2006. Probabilistic service life assessment and maintenance planning of concrete structures. *Journal of Structural Engineering*, ASCE, 132(5), 810–825.

Biondini, F. & Frangopol, D.M. 2009. Lifetime reliability based optimization of reinforced concrete cross-sections under corrosion. *Structural Safety*, 31, 483–489.

Biondini, F., 2009. A Measure of Lifetime Structural Robustness, *Structures Congress*, ASCE/SEI, Austin, TX, USA, April 29-May 3.

Biondini, F., Palermo, A. & Toniolo, G. 2011. Seismic performance of concrete structures exposed to corrosion: Case studies of low-rise precast buildings. *Structure and Infrastructure Engineering*, 7(1–2), 109–119.

Biondini, F., Camnasio, E. & Palermo, A. 2013. Lifetime seismic performance of concrete bridges exposed to corrosion. *Structure and Infrastructure Engineering*, DOI: 10.1080/15732479.2012.761248 (In press).

Bocchini, P. & Frangopol, D.M. 2012. Restoration of bridge networks after an earthquake: multicriteria intervention optimization. *Earthquake Spectra*, 28(1), 427–455.

Bocchini, P., Decò, A. & Frangopol, D.M. 2012. Probabilistic functionality recovery model for resilience analysis. *Sixth Int. Conf. of Bridge Maintenance, Safety and Management* (IABMAS 2012), Stresa, Italy, July 8–12, 2012. In: F. Biondini & D.M. Frangopol (Eds.), *Bridge Maintenance, Safety, Management, Resilience and Sustainability*. CRC Press/Balkema, Taylor and Francis Group, London, UK.

Bruneau, M., Chang, S.E., Eguchi, R.T., Lee, G.C., Tierney, K., Wallace, W.A. & Wintefeldt, D.V. 2003. A framework to quantitatively assess and enhance the seismic resilience of communities. *Earthquake Spectra*, 19(4), 733–752.

Bruneau, M. & Reinhorn, A.M. 2007. Exploring the concept of seismic resilience for acute care facilities. *Earthquake Spectra*, 23(1), 41–62.

CEN-EN 1998-1 2004. *Eurocode 8: design of structures for earthquake resistance – part 1: general rules, seismic actions and rules for buildings*. European Committee for Standardization, Brussels.

Chang, S.E. & Shinozuka, M. 2004. Measuring improvements in the disaster resilience of communities. *Earthquake Spectra*, 20(3), 739–755.

Cimellaro, G.P., Reinhorn, A.M. & Bruneau, M. 2010a. Framework for analytical quantification of disaster resilience. *Engineering Structures,* 32(11), 3639–3649.

Cimellaro, G.P., Reinhorn, A.M. & Bruneau, M. 2010b. Seismic resilience of a hospital system. *Structure and Infrastructure Engineering,* 6(1–2), 127–144.

Decò, A., Bocchini, P. & Frangopol, D.M. 2013. A probabilistic approach for the prediction of seismic resilience of bridges. *Earthquake Engineering and Structural Dynamics*, DOI: 10.1002/eqe.2282 (In press).

Dolšek, M. 2009. Incremental dynamic analysis with consideration of modeling uncertainties. *Earthquake Engineering and Structural Dynamics,* 38(6), 805–825.

Dolšek, M. 2011. Simplified method for seismic risk assessment of buildings with consideration of aleatory and epistemic uncertainty. *Structure and Infrastructure Engineering,* 8(10), 939–953.

Fajfar, P. 1999. Capacity spectrum method based on inelastic demand spectra. *Earthquake Engineering and Structural Dynamics*, 28(9), 979–993.

Frangopol, D.M. & Curley, J.P. 1987. Effects of Damage and Redundancy on Structural Reliability. *Journal of Structural Engineering*, ASCE, 113(7), 1533–1549.

Glicksman, M. E. 2000. *Diffusion in solids*, John Wiley and Sons.

Haselton, C. 2006. *Assessing seismic collapse safety of modern reinforced concrete moment frame buildings*. PhD thesis, Stanford University, Stanford, CA, USA.

Ibarra, L., Medina, R. & Krawinkler, H. 2005. Hysteretic models that incorporate strength and stiffness deterioration. *Earthquake Engineering and Structural Dynamics*, 34(12), 1489–1511.

Iman, R.L. & Conover, W.J. 1982. A distribution-free approach to inducing rank correlation among input variables. *Communication in Statistics,* 11(3), 311–334.

Kafali, C. & Grigoriu, M. 2005. Rehabilitation decision analysis, *9th Int. Conf. on Structural Safety and Reliability* (ICOSSAR'05), Rome, Italy, June 19–23, 2005. In: G. Augusti, G. Schuëller & M. Ciampoli (Eds.), *Safety and Reliability of Engineering Systems and Structures*, Millpress, 2773–2780.

Pastore, T., Pedeferri, P., 1994. La corrosione e la protezione delle opere metalliche esposte all'atmosfera, *L'edilizia*, December, 1994, 75–92 (In Italian).

Titi, A. 2012. *Lifetime probabilistic seismic assessment of multi-storey precast buildings*. PhD thesis, Politecnico di Milano, Milan, Italy.

Vořechovský, M. & Novák, D. 2009. Correlation control in small-sample Monte Carlo type simulations I: A simulated annealing approach. *Probabilistic Engineering Mechanics*, 24(3), 452–462.